A Connection Between Star Formation Rate and Dark Matter Halos at $Z \sim 6$ In 2013 Planck Cosmology.

F.L. Gómez-Cortés[1]

Departamento de Fsica, Universidad de los Andes, Colombia

Received _____; accepted _____

ABSTRACT

This work relates baryonic matter and dark matter at redshift $z = 5.9$ using observational data from CFHTLS (Willott 2013), HUDF09 (Bouwens 2006, 2012), UKIDSS and SDXS (McLure 2009), and results of the Multidark Simulation (Riebe 2013) in a cubic box of 1000Mpc h^{-1} length with 2013 Planck Cosmology. The Luminosity Function (LF) is fitted via four parameters with the Markov Chain Monte Carlo method. The relationship between the Dark Matter Halos Mass and Star Formation Rate is obtained using the relationship between the UV continuum (from the fitted LF) and Star Formation Rate (SFR) by Kennicutt (1998).Cosmic variance effects are studied on smaller boxes of 250Mpc h^{-1} length.

Halos.

Subject headings: Dark Matter, LF, SFR, High Redshift Galaxies, Reionization

1. Introduction

Dark matter is a significative component of the universe.

(Trimble 1987)

Hierarchy Structure Evolution: Early formation of small structures merging on major structures after.

From simulations, Halo Mass Function as function of redshift (or time).

Star formation rate as function of time. Peak at $z \sim 2$.

Main Objetive: Reproduce the observed luminosity function at redshift $z = 5.9$ from a DMH catalog from simulations.

1.1. Halo Mass Function (HMF)

1.2. Cosmic Variance

2. Linking Galaxy Luminosity Function (GLF) and Dark Matter Halo (DMH) mass

2.1. Magnitude to Luminosity

Luminosity Functions (LF) are usually expressed in terms of magnitude instead luminosity. Luminosity is the energy emmited by a source in a given wavelengt range, is a physical quantity. Magnitude is a classification inherited from ancient Greeks, this quantifies the response of the first astrometric device: the human eye, this perception grows loarithmically with the retrieved radiation.

Luminosity of any object can be compared with Sun Luminosity ($L_{\lambda\odot}$) at any

wavelengt. With the Sun Magnitude as reference ($M_{\lambda\odot}$), the absolute magnitud of the objet at an specific wavelengt is given by:

$$M_\lambda = M_{\lambda\odot} - 2.5 \log_{10}\left(\frac{L_\lambda}{L_{\lambda\odot}}\right)$$

The solar absolute magnitude in the U filter is $M_{U\odot} = 5.61$, and the solar luminosity in the same filter is $L_{U\odot} = 10^{18.48}$ergs s^{-1}Hz^{-1} or $L_{U\odot} = 3.02 \times 10^{18}$ergs s^{-1}Hz^{-1}. The solar luminosity can be used as refference unit, in this fashion, the typical luminosity of a galaxy can be expresed in terms of $10^8 - 10^{11}$ times the sun luminosity.

The absolute magnitude of a galaxy equation in the U filter:

$$M_U = 51.82 - 2.5 \log_{10}(L_U)$$

2.2. The Luminosity Model

In this model we have made two assumptions:

1. Each halo in the catalog hosts one galaxy. There are not empty halos, also none of halos has two or more galaxies.

2. The UV luminosity of each galaxy is function of one variable: the mass of the DMH in wich is located.

The simplest relation we can have is a powerlaw:

$$L = L_0 M^{\alpha} \tag{1}$$

but has not well agreement with observed luminosity functions.

A better model is a four parameter function. Each galaxy has a luminosity given by:

$$L = L_0 M \left[\left(\frac{M}{M_0} \right)^{-\beta} + \left(\frac{M}{M_0} \right)^{\gamma} \right]^{-1} \tag{2}$$

where M is the hosting DMH mass, L_0 is a normalization constant, M_0 is the critical mass where the luminosity function has a slope change, β and γ are the slopes. This equation has a similar fashion to the mass to light relation (van den Bosch 203) and the mean relation between stellar mas of a galaxy and the mas of its halo used by Moster (2010).

There are more complex models(Lee 2009) that includes a random behavior: galaxies has not synchronization on the beginning of star forming stage, also this stage may be time limited. This is called duty cycle. It is probable to have in the observations some invisible galaxies in the UV continuum due their duty cycle may has not started as well it may ended. Also may be present a normal distribution of the luminosity around the expected values.

2.3. Star Formation Rate

On the study of far galaxies individual stellar spectrum is unresolved, is not possible to make a detailed census of the galaxy popullation. Only is possible to get information from the whole stellar population, an integrated spectrum.

Kennicutt pruposed a method in wich a linear relation between luminosity and SFR can be assumed. This model allows to estimate the young stars fraction and the mean SFR over periods of $10^8 - 10^9$yr. The luminosity in the modfel, comes from the UV and the FIR broadband, also from speciffic recombination lines.

In a typical galaxy spectrum the visible wavelengths are dominated by the main sequence stars (A to early F) and G-K giants. In few wavelength ranges we have a significative contribution from the young stars rather than the old stars. The infrared and far infrared wavelengths emission is dominated by dust, this dust is heated by the whole stellar popullation, in particular by young, UV-bright stars (Law 2011).The UV broadband emission is dominated by blue stars with temperature near to 40.000K. These hot and massive stars has a lifetime of 10^8Gyr, they spend their nuclear fuel faster than smaller and cooler sunlike stars.

The relation between UV luminosity and Star Formation Rate (Kennicutt 1998) is given by: $\mathrm{SFR}\,(M_\odot \mathrm{yr}^{-1}) = 1.4 \times 10^{28} L_\nu \left(\mathrm{erg\ s^{-1}Hz^{-1}}\right)$ With Initial Mass Function (IMF) between $0.1M_\odot$ and $100M_\odot$, in the range of $1250 - 2500$Å

The UV dust absorption (Kennicutt 2009) is not taken account in this work.

DUST EXTINTION ALSO STUDIED by 002-TACCHELLA-A Physical Model for —

3. Observations

The dataset was retrieved from graphs for Bouwens (2014) and McLure (2009) using DEXTER http://dc.zah.uni-heidelberg.de/dexter/ui/ui/custom

3.1. CFHTLS

CFHTLS - Canada-France-Hawaii Telescope Legacy Survey - MegaCam(Willott 2013)

"We identify a sample of 40 Lyman break galaxies brighter than magnitude z = 25.3 across an area of almost 4 square degrees. Sensitive spectroscopic observations of seven galaxies provide redshifts for four, of which only two have moderate to strong Ly emission lines. All four have clear continuum breaks in their spectra." Willott (2013).

"The imaging data used to select high-redshift galax- ies come primarily from the 3.6 m Canada-France-Hawaii Telescope. Optical observations with MegaCam in the u g r i z filters are from CFHTLS Deep which covered four 1 square degree fields with typical total integra- tion time of 75 ks in u , 85 ks in g , 145 ks in r , 230 ks in i and 175 ks in z . The seeing in the final stacks at i and z range from 0.66 to 0.76 arcsec. The data used here are from the 6th data release, T0006, which contains all the data acquired over the five years of the project " Willott (2013).

"These optical data are complemented by near-IR data from the WIRCam Deep Survey (WIRDS; Bielby et al. 2012). WIRDS used the WIRCam near-IR imager at the CFHT" Willott (2013).

About the Luminosity function: sect 6.3 "Because our LBG sample covers only a limited range of apparent and absolute magnitudes, we cannot use it to determine the full galaxy luminosity function at z = 6. The luminosity function at the break and at fainter

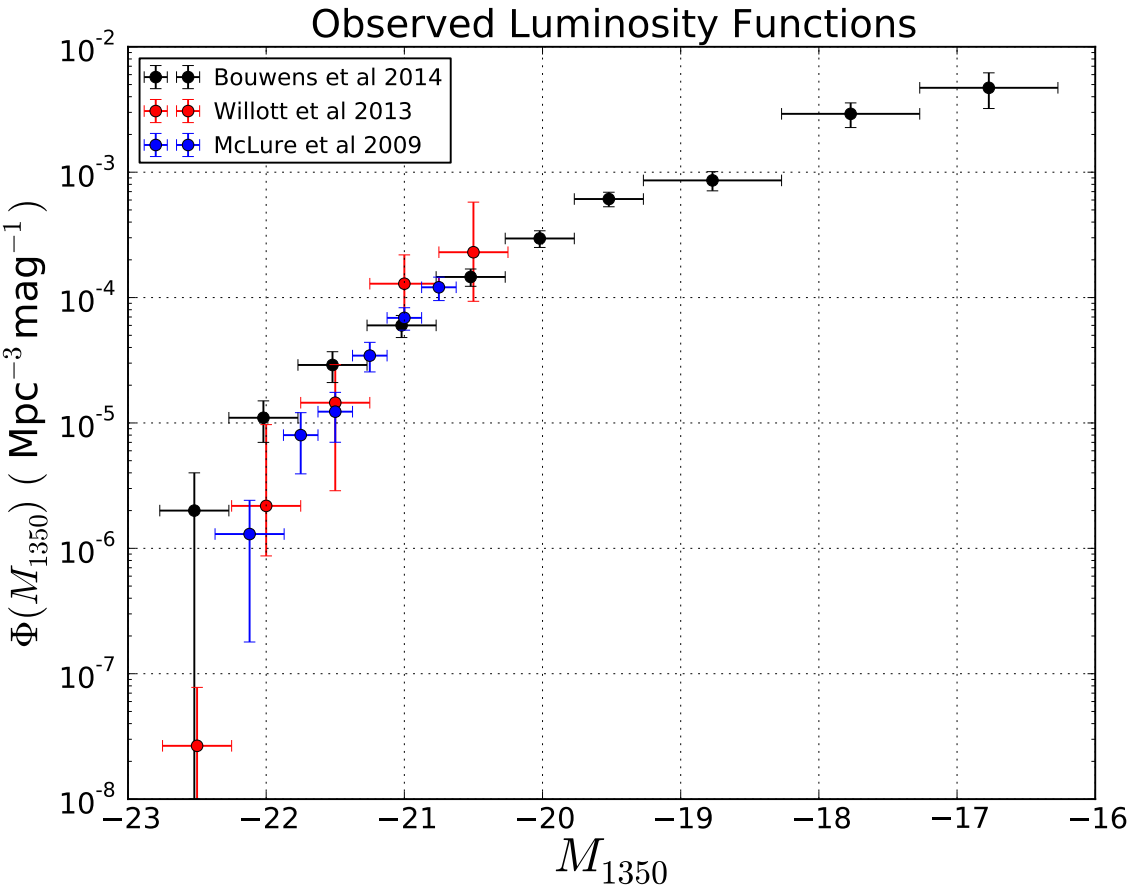

Fig. 1.— Observational data from Bouwens (2014); McLure (2009)and Willott (2013).

magnitudes has already been well studied from deep HST surveys over small sky areas (Bouwens et al. 2007). The main contribution of our study is to determine the space density of very rare, highly luminous LBGs."Willott (2013).

3.2. HUDF09

"Table 1 summarizes the search fields used for the z 5- 8 LF determinations and the approximate depths of the available ACS+WFC3/IR observations. Our primary data set consists of the full two-year WFC3/IR obser- vations of the HUDF and two flanking fields obtained with the 192-orbit HUDF09 program (PI Illingworth: GO 11563). Our second data set is the 145 arcmin 2 ACS+WFC3/IR observations over the wide-area Early Release Science (Windhorst et al. 2011) and CDF-South CANDELS" Bouwens (2012)

"A detailed summary of the ACS HUDF, HUDF-Ps, and GOODS data we use for our dropout selections is provided in our previous work (B06). Nevertheless, a brief description of the data is in- cluded here. The ACS HUDF data we use are the version 1.0 re- ductions of Beckwith et al. (2006) and extend to 5 point-source limits of 29Y30 in the B 435 V 606 i 775 z 850 bands. The HUDF-Ps re- ductions we use are from B06 and take advantage of the deep (k72 orbit) BViz ACS data fields taken in parallel with the HUDF NICMOS program (Thompson et al. 2005). Together the parallel data from this program sum to create two very deep ACS fields that we can use for dropout searches. While of somewhat var- iable depths, the central portions of these fields (12Y20 arcmin 2) reach some 0.6Y0.9 mag deeper than the data in the original ACS GOODS program (Giavalisco et al. 2004a). Finally, for the ACS GOODS reductions, we use an updated version of those generated for our previous z 6 study (B06)." Bouwens (2006)

3.3. UKIDSS & SDXS

"The UDS is the deepest of five near-IR surveys currently underway at the UK InfraRed Telescope (UKIRT) with the new WFCAM imager (Casali et al. 2007) which together comprise the UKIDSS (Lawrence et al. 2007). The UDS covers an area of 0.8 deg 2 cen- tred on RA = 02:17:48, Dec. = 05:05:57 (J2000) and is already the deepest, large area, near-IR survey ever undertaken. The data utilized in this paper were taken from the first UKIDSS Data Re- lease (DR1; Warren et al. 2007), which included JK imaging of the entire UDS field to 5 depths of J = 23.9, K = 23.8 (1.6 arcsec diameter apertures). The UKIDSS DR1 became publicly available to the world wide astronomical community in 2008 January and can be downloaded from the WFCAM Science Archive. 2 The UDS field is covered by a wide variety of deep, multiwave- length observations ranging from the X-ray through to the radio (see Cirasuolo et al. 2008 for a recent summary). However, for this study the most important multiwavelength observations are the deep op- tical imaging of the field taken with Suprime-Cam (Miyazaki et al. 2002) on Subaru as part of the Subaru/XMMNewton Deep Survey (Sekiguchi et al. 2005). The optical imaging consists of five over- lapping Suprime-Cam pointings, and covers an area of 1.3 deg 2 . The whole field has been imaged in the BV Ri z filters, to typical 5 depths of B = 27.9, V = 27.4, R = 27.2, i = 27.2 and z = 26.2 (1.6 arcsec diameter apertures). The reduced optical imaging of the SXDS is now publicly available 3 and full details of the observations, data reduction and calibration procedures are provided in Furusawa et al. (2008). The high-redshift galaxies investigated in this study were selected from a contiguous area of 0.63 deg 2 (excluding areas contaminated by bright stars and CCD blooming) covered by both the UDS near-IR and SXDS optical imaging." McLure (2009)

3.4. The Drop-out Technique - Lyman Break Technique

Steidel (2003)

4. Discussion

Q: Mpc/h ?

(Lundgren 2914(@) SFR evolution from $z = 1$ to 6

(Bouwens 2014) HST Legacy

(Jiang 2011) Keck pectroscopy

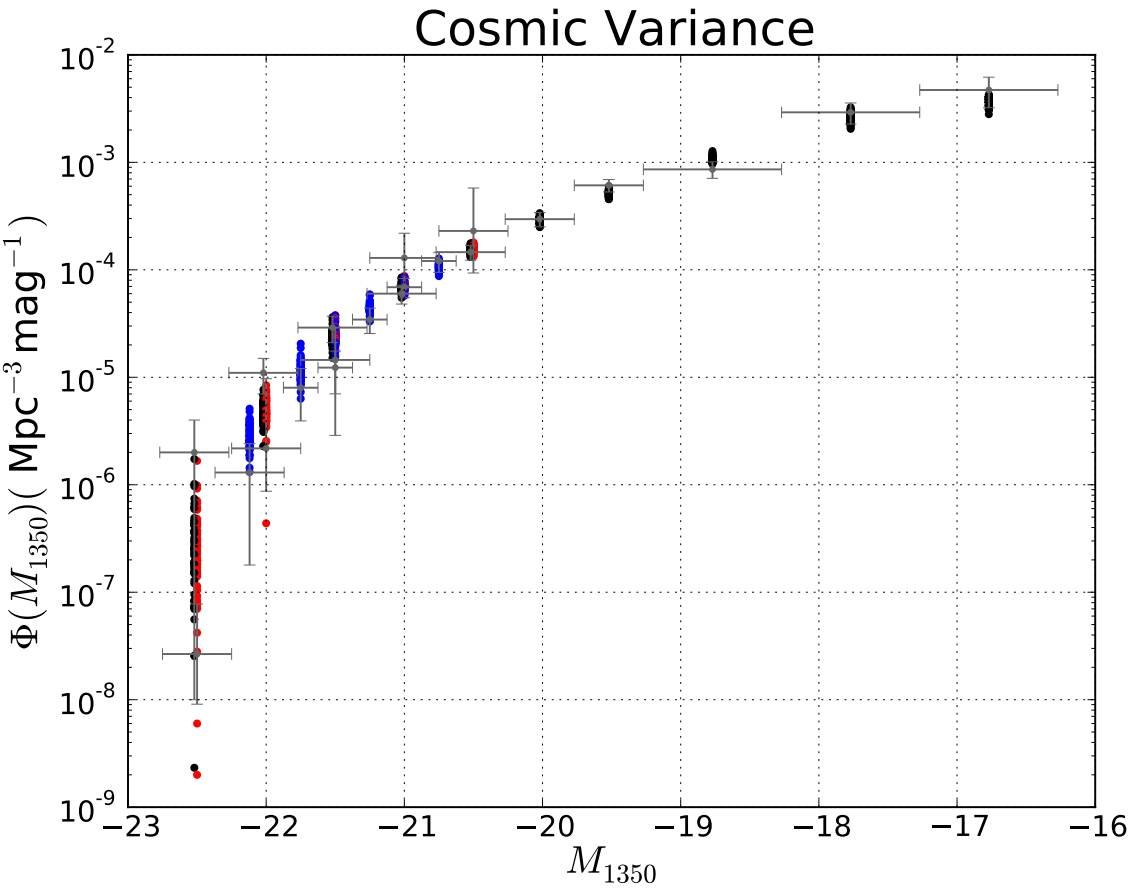

Fig. 2.— Cosmic Variance: The Luminosity Function is made using the DMH catalog from the full box and the set of parameters from the small boxes.

5. Summary

A. Appendix material

DEXTER http://dc.zah.uni-heidelberg.de/dexter/ui/ui/custom

REFERENCES

Bouwens, R. J. et al. 2006, ApJ, 653, 53

Bouwens, R. J. et al. 2012, ApJ, 752, 5

Bouwens, R. J. et al. 2012, arXiv:1403.4295

Kennicutt, Robert C., Jr. 1998, ARA&A, 36, 189

Kennicutt, Robert C., Jr et al. 2009, ApJ, 703, 4672

Law, K. et al. 2011, ApJ, 738, 124

Jiang, Linhua et al. 2011, ApJ, 743, 65

Lee, Kyoung-Soo et al. 2009, ApJ, 695, 368

Lundgren, Britt F. et al, 2014, ApJ, 780,34

McLure, R. J. et al. 2009, MNRAS, 395, 2196

Moster, Benjamin P. et al. 2010, ApJ, 710, 903

Riebe, K. et al. 2013, AN, 334, 691

Steidel, Charles C. et al. 2003, ApJ, 592, 728

Trible, Virginia. 1987, ARA&A, 25, 425

van den Bosh, Frank C. et al. 2003, MNRAS, 40, 771

Willott, Chris J. et al. 2013, AJ, 145, 4